Atmospheric Research 297 (2024) 107126

Contents lists available at ScienceDirect

Atmospheric Research

journal homepage: www.elsevier.com/locate/atmosres

Observed impacts of the North Pacific Victoria Mode on Indian summer monsoon onset

Suqin Zhang [a,b,f], Peng Hu [c,d,*], Gang Huang [a,b,f,*], Xia Qu [a,e]

[a] State Key Laboratory of Numerical Modeling for Atmospheric Sciences and Geophysical Fluid Dynamics, Institute of Atmospheric Physics, Chinese Academy of Sciences, Beijing 100029, China
[b] Laboratory for Regional Oceanography and Numerical Modeling, Qingdao National Laboratory for Marine Science and Technology, Qingdao 266237, China
[c] Yunnan Key Laboratory of Meteorological Disasters and Climate Resources in the Greater Mekong Subregion, Yunnan University, Kunming 650091, China
[d] Department of Atmospheric Sciences, Yunnan University, Kunming 650500, China
[e] Center for Monsoon System Research, Institute of Atmospheric Physics, Chinese Academy of Sciences, Beijing 100029, China
[f] University of Chinese Academy of Sciences, Beijing 100049, China

ARTICLE INFO

Keywords:
India summer monsoon
Monsoon onset
Victoria Mode
Rossby wave train
El Niño-Southern Oscillation

ABSTRACT

The onset of the Indian summer monsoon (ISM) marks the arrival of the rainy season and affects billions of people. Therefore, exploring the factors influencing ISM onset is essential, especially sea surface temperature (SST) anomalies. In addition to the well-known El Niño-Southern Oscillation in the tropical Pacific, in this study, we find that the SST anomalies in the extratropical Pacific (Victoria mode, VM) can significantly impact ISM onset. The positive phase of the May VM causes monsoon onset delay, and two distinct mechanisms linking these phenomena are identified. The tropical pathway involves divergent circulation and equatorial Rossby waves. The VM-associated SST gradient causes low-level divergence and suppressed rainfall around the Indo-China Peninsula. Such suppressed rainfall induces anomalous anticyclone circulation by exciting the equatorial Rossby wave response, which prevents the establishment of monsoonal southwesterly winds and moisture transport, therefore delaying ISM onset. The extratropical pathway involves the Rossby wave train and land–sea thermal contrast. The VM triggers an eastward Rossby wave train via upper-level divergence around the Gulf of Alaska. This wave train propagates downstream and generates anomalous negative geopotential heights and low air temperatures to the northwest of India, which reduces the land–sea thermal contrast and delays ISM onset. Our result suggest that the ISM onset predictions should consider the role of May VM.

1. Introduction

The onset of the Indian summer monsoon (ISM) marks the end of the hot season and the beginning of the rainy season, which is critical to the lives of billions of people (Joseph et al., 2006; Pai and Rajeevan, 2009; Wang et al., 2009; Bombardi et al., 2020; Hu et al., 2022a). Advanced or delayed ISM onset could lead to drastic floods or droughts, respectively, thus affecting water management, energy generation, agricultural production, and human health (Noska and Misra, 2016; Bombardi et al., 2019; Bombardi et al., 2020). Over the past eighty years, numerous studies have been devoted to investigating the multi-timescale factors that influence ISM onset (Wang et al., 2009; Bombardi et al., 2020; Hu et al., 2022a; and references therein). For example, synoptic-scale disturbances such as monsoon onset vortices and Arabian Sea cyclones are direct triggers of ISM onset (Krishnamurti et al., 1981; Deepa and Oh, 2014; Baburaj et al., 2022b; Sasanka et al., 2023). At the intraseasonal timescale, ISM onset tends to occur during the wet phase of the quasi-biweekly oscillation (Wang et al., 2009; Lee et al., 2013; Qian et al., 2019) and the 30–60-day oscillation (Wheeler and Hendon, 2004; Wang et al., 2009; Kikuchi, 2021; Baburaj et al., 2022a; Lenka et al., 2023a, 2023b). On interannual-to-interdecadal timescales, ISM onset is modulated by sea surface temperature (SST) anomalies over the Pacific Ocean, including the Pacific Decadal Oscillation (PDO; Xiang and Wang, 2013; Watanabe and Yamazaki, 2014; Hu et al., 2022a; Hu et al., 2023) and the El Niño-Southern Oscillation (ENSO). Although multiple factors have been identified, the forecasting skill of the ISM onset date remains to be improved (Goswami and Gouda, 2010; Gouda et al., 2021).

Fig. 1a shows the correlation between ISM onset and SST anomalies

* Corresponding authors at: Yunnan Key Laboratory of Meteorological Disasters and Climate Resources in the Greater Mekong Subregion, Yunnan University, Kunming 650091, China.
E-mail addresses: hupeng@mail.iap.ac.cn (P. Hu), hg@mail.iap.ac.cn (G. Huang).

https://doi.org/10.1016/j.atmosres.2023.107126
Received 15 August 2023; Received in revised form 21 October 2023; Accepted 20 November 2023
Available online 26 November 2023

in the preceding winter. Typically, a wintertime El Niño event tends to be followed by delayed ISM onset, and the opposite is often true for a La Niña event (Joseph et al., 2006; Ordoñez et al., 2016; Preenu et al., 2017; Hu et al., 2022a). Previous studies have revealed various pathways through which the ENSO modulates monsoon onset (Fig. 1b), including the tropical tropospheric temperature (Chiang and Sobel, 2002; Zhang et al., 2016; Hu et al., 2021), the Walker circulation (Wang et al., 2017; Wu and Mao, 2019; Hu et al., 2022a), and the western North Pacific (WNP) anticyclone (Xie et al., 2016; Li et al., 2017; Zhang et al., 2017). For instance, significant warming of the tropical troposphere in response to El Niño convections can reduce the climatological land–sea thermal contrast, leading to delayed ISM onset (Fig. 1c). Furthermore, the SST gradient in the tropical Pacific induces a descending motion and low-level divergence in the WNP, known as the Walker circulation (Fig. 1c). Because of its geographical location, such descent and divergence may more directly affect monsoon onset over the South China Sea than over India (Hu et al., 2020; Hu et al., 2022a; Hu et al., 2022b). However, the Walker circulation can also contribute to the WNP anticyclone (Wang et al., 2000; Xie et al., 2016; Li et al., 2017) and thus indirectly modulate ISM onset. Specifically, the anomalous easterly winds to the south of the WNP anticyclone can extend westward and reach the northern Indian Ocean (Xie et al., 2016; Hu et al., 2022a; Hu et al., 2023). Such easterly winds hinder the firm establishment of monsoonal southwesterly winds, thus leading to delayed ISM onset (Fig. 1d). In summary, by modulating the above three tropical pathways (tropospheric temperature, Walker circulation, and WNP anticyclone), the preceding El Niño (La Niña) event exhibits an in-phase relationship with Indian summer monsoon onset, which tends to be delayed (advanced) after El Niño (La Niña) event occurrence.

In addition to tropical SST anomalies such as the ENSO, extratropical SST anomalies may modulate monsoon onset (Fig. 1a; Hu et al., 2022a; Hu et al., 2022b; Hu et al., 2023). SST anomalies in the North Pacific (poleward of 20°N) mainly consist of two dominant modes: the PDO and the Victoria Mode (VM). Given the similarities in the spatial structure between the ENSO and PDO, the latter can also influence monsoon onset via tropical pathways such as the tropospheric temperature (Hu et al., 2022a; Hu et al., 2023). However, compared to the equatorially confined SST anomalies associated with the ENSO, the PDO exhibits a stronger signal in the extratropical North Pacific (Deser et al., 2010; Newman et al., 2016; Liu and Di, 2018). In recent studies, it has been suggested that the PDO modulates monsoon onset by exciting an extratropical Rossby wave train (Hu et al., 2022a; Hu et al., 2023). Such a Rossby wave train is closely related to vertical motion and SST anomalies in the subtropical North Pacific and exhibits strong interactions with the basic flow and synoptic-scale eddies (Hu et al., 2022a; Hu et al., 2023).

Orthogonal to and independent of the PDO, the VM is the second dominant mode of North Pacific variability (Ding et al., 2015; Pu et al., 2019; Zou et al., 2020; Hu et al., 2022b). Closely linked to the North Pacific Oscillation and thermal forcing over the Tibetan Plateau, the VM features a tripole-like anomalous SST pattern in the extratropical North Pacific (Bond et al., 2003; Ding et al., 2015; Chen et al., 2021; Yu et al., 2022). In previous studies, the wide-ranging climate impacts of the VM have been documented, for example, subsequently triggering the ENSO through the seasonal footprint mechanism and the trade wind charging mechanism (Ding et al., 2015; Li et al., 2019; Ding et al., 2022; Ji et al., 2023). The VM can also influence tropical cyclone activity over the WNP (Zhang et al., 2013; Pu et al., 2019; Dai et al., 2022), winter precipitation over South China (Zou et al., 2020), the location of the South Asian high (Yang et al., 2022), and the intensity and onset of the South China Sea summer monsoon (Ding et al., 2018; Hu et al., 2022b; Chen et al., 2023).

However, in contrast to the ENSO and PDO (Hu et al., 2022a; Hu et al., 2023; and references therein), the impacts of the North Pacific VM on ISM onset remain elusive. The VM, similar to the PDO, exhibits significant SST anomalies in the extratropical North Pacific. Could the VM also influence monsoon onset by exciting a Rossby wave train? This is the scientific question we aim to answer. The rest of this study is organized as follows: in Section 2, the datasets and methods are described.

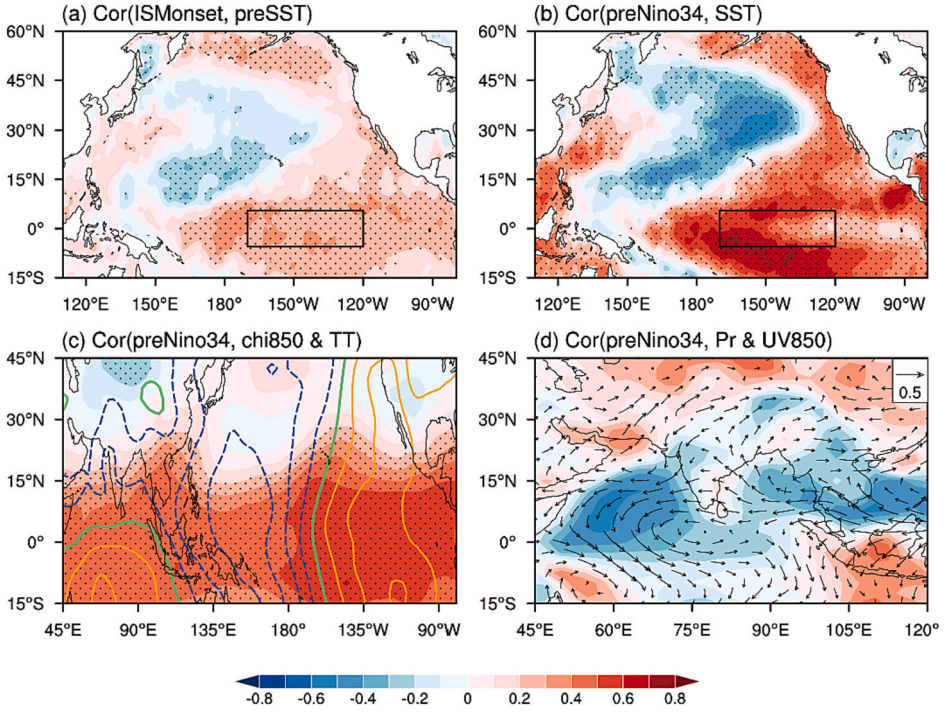

Fig. 1. The impacts of preceding winter ENSO on the following ISM onset. **(a)** The correlation between ISM onset and the SST anomalies in the preceding winter (DJF). **(b)** The correlation between the preceding winter Niño3.4 index and the following May SST anomalies. **(c)** The correlation between the preceding winter Niño3.4 index and velocity potential at 850 hPa (contours) and tropospheric temperature (shadings). **(d)** The correlation between the preceding winter Niño3.4 index and precipitation (shadings) and winds at 850 hPa (vectors). The dots region indicates the correlation is significant at the 90% confidence level. The black rectangles highlight the key area of the Niño3.4 index (5°S–5°N, 120°–170°W).

The statistical relationship and dynamic mechanisms between the VM and ISM onset are investigated in Section 3. Finally, a summary and discussion are presented in Section 4.

2. Data and methods

The onset date of the ISM was derived from the Indian Meteorological Department (Ananthakrishnan and Soman, 1988; Joseph et al., 1994; Wang et al., 2009), which mainly emphasizes the sharp and sustained increase in rainfall over Kerala (located in southwestern India). However, local rainfall can be contaminated by small-scale disturbances unrelated to large-scale monsoonal circulation, which may result in a "bogus" monsoon onset (Wang et al., 2009; Ordoñez et al., 2016). As such, in recent years, the Indian Meteorological Department adopted the objective methods proposed by Joseph et al. (2006) and Pai and Rajeevan (2009), which also consider the occurrence of active convection and the establishment of monsoonal flow. The mean ISM onset date from 1948 to 2022 is May 31, and the standard deviation is 7.3 days. Following previous studies on ISM onset (Xiang and Wang, 2013; Watanabe and Yamazaki, 2014; Hu et al., 2023), in this study, we mainly focused on the monthly mean field of May, the transition month of the Asian summer monsoon.

The monthly mean reanalysis and observational datasets employed in this study include: (a) National Centers for Environmental Prediction/National Center for Atmospheric Research (NCEP/NCAR) reanalysis data with a horizontal resolution of 2.5° × 2.5° (Kalnay et al., 1996); (b) Precipitation Reconstruction (PREC) data with a horizontal resolution of 2.5° × 2.5° (Chen et al., 2002); and (c) Hadley Centre Global Sea Ice and Sea Surface Temperature (HadISST) data with a horizontal resolution of 1.0° × 1.0° (Rayner et al., 2003). All the above datasets cover the analysis period of 75 years (1948–2022). Following previous studies (e.g., Bond et al. (2003) and Ding et al. (2015)), the VM is defined as the second dominant mode of North Pacific SST anomalies (i.e., EOF2), and the corresponding principal component is regarded as the VM index (i.e., PC2). The statistical significance of the linear correlation and regression are estimated by the two-sided Student's *t*-test (Wilks, 2019).

In the previous studies, it have been noted that a reduced meridional land–sea thermal contrast tends to delay ISM onset (e.g., Watanabe and Yamazaki, 2014). Through the analysis of the extratropical Rossby wave train pathway, it is found that the May North Pacific VM could cool the airmass over northwestern India to modify the land–sea thermal contrast, as described in Section 3.2. Therefore, conforming with previous studies (Bawiskar, 2009; Liu and Zhu, 2021; Lenka et al., 2023a), the tropospheric temperature gradient (TTG) is defined to characterize the meridional sea–land thermal contrast:

$$TTG = \partial_y(TT) \tag{1}$$

where TT is the troposphere temperature, i.e., the vertically averaged air temperature from 850 to 200 hPa. $TTG < 0$ indicates a reduced land–sea thermal contrast.

To investigate the steady atmospheric response to divergence forcing, the linear baroclinic model (LBM) is employed in this study (Watanabe and Kimoto, 2000; Zhang et al., 2023). The LBM has a horizontal resolution of T42 and vertical 20 sigma levels. The May climatology from 1981 to 2010 is used as the background. In this work, the LBM is integrated for 34 days by the time integration method, and the average data from 25 to 34 days are considered the steady response.

3. Impact of the North Pacific VM on ISM onset

3.1. Statistical relationship between the VM and ISM onset

Fig. 2a shows the correlation coefficient between the ISM onset date and the SST anomalies in May. Corresponding to delayed monsoon onset, significant warm SST anomalies emerge in the equatorial central Pacific, which resemble the decaying phase of an El Niño event and are consistent with previous studies (Hu et al., 2022a). Moreover, cold SST

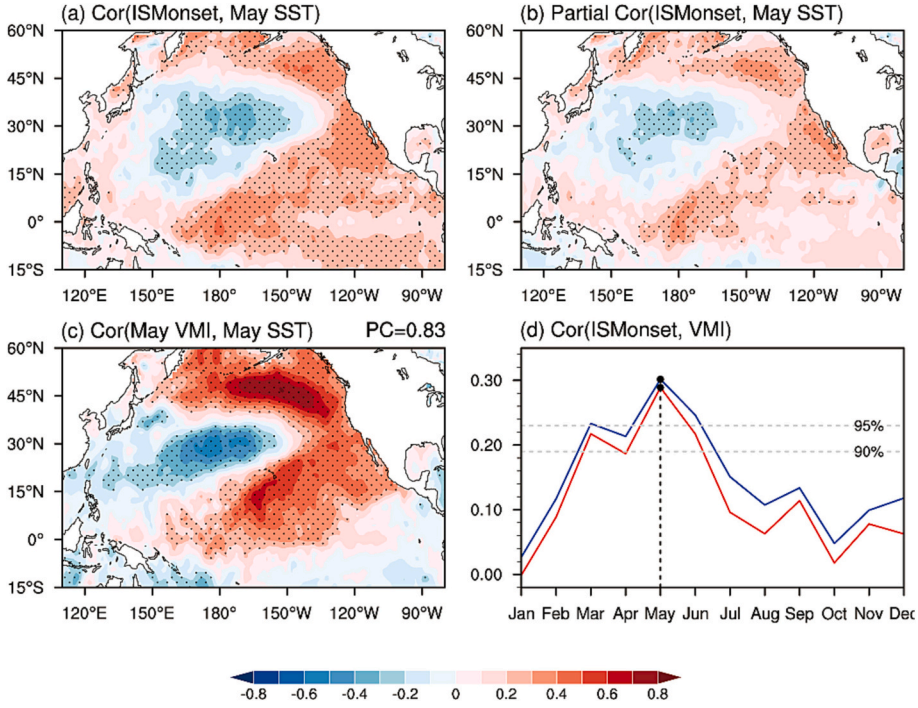

Fig. 2. The correlation coefficient between **(a)** the ISM onset date and the SST anomalies in May, **(c)** May VM index and SST anomalies. **(b)** The same as (a), but removing the preceding winter Niño3.4 index. The spatial correlation coefficient between (b) and (c) is shown in the upper-right corner of (c). **(d)** The correlation coefficient between the ISM onset date and VM index (blue line), and the partial correlation between them after removing the preceding winter Niño3.4 index (red line). The horizontal gray dashed lines indicate the 90% and 95% confidence levels. The dots denote the correlation coefficient passing the 90% confidence level. (For interpretation of the references to colour in this figure legend, the reader is referred to the web version of this article.)

anomalies are highly evident in the subtropical North Pacific and are even more pronounced than those in the preceding winter (Fig. 1a). To remove the signals of the wintertime ENSO, Fig. 2b further shows the partial correlation between the monsoon onset date and SST anomalies. While the SST anomalies in the equatorial central-eastern Pacific are no longer significant, tripole-like SST anomalies still remain in the North Pacific. Such North Pacific SST anomalies resemble the canonical structure of the VM shown in Fig. 2c, with a spatial correlation coefficient of 0.83. This SST pattern features significant cold SST anomalies approximately 20°-35°N surrounded by warm SST anomalies to the south (5°-20°N) and north (45°-60°N). The close linkage between ISM onset and the VM is further confirmed in Fig. 2d, which shows the correlation between the monsoon onset date and the VM index in each month. While ISM onset is significantly correlated with the VM index in the springtime (March–April-May), the correlation coefficient is the highest in May. As such, in this study, we mainly focused on circulation anomalies in May, consistent with previous studies on ISM onset (Watanabe and Yamazaki, 2014; Hu et al., 2023). Notably, the correlation between the VM and ISM onset is largely independent of the occurrence of a preceding ENSO event, as revealed by the partial correlation shown in Fig. 2d.

The normalized time series of ISM onset and the VM index in May is shown in Fig. 3. For comparison, the normalized Niño 3.4 index in the preceding winter is also presented. Overall, the preceding ENSO and VM in May exhibit an in-phase variation with ISM onset. The correlation coefficient of ISM onset with the ENSO is 0.291 and with the VM is 0.288, which is significant at the 95% confidence level. Moreover, the linkage between the wintertime ENSO and VM in May is very weak, with a correlation coefficient of −0.04. This result suggests that the importance of the VM for ISM onset is comparable to that of the ENSO, and the VM is largely independent of the preceding ENSO. To avoid the influence of global warming on the shift in onset dates, a 9-year highpass filter is applied to the ISM onset date and the VM index in May, and the results are shown in Fig. S1. After removing the long-term trend and the interdecadal background, the interannual relationship between ISM onset and the VM in May remains very notable, with a correlation coefficient of 0.38, which is significant at the 99% confidence level. Therefore, the VM in the North Pacific may be used as an independent and major factor in influencing and forecasting ISM onset.

The close linkage between the North Pacific VM and ISM onset is further confirmed in Fig. 4a, which shows the correlation between the VM index and rainfall as well as low-level circulation in May. Corresponding to the positive phase of the VM, reduced rainfall emerges in the Arabian Sea, Bay of Bengal, and Indo-China Peninsula. In addition, an anomalous anticyclone is observed in the North Indian Ocean, with anomalous easterly winds extending from the Bay of Bengal to the Arabian Sea. Notably, the anomalous anticyclone is located to the west of the observed reduced rainfall, which can be considered as the equatorial Rossby wave response to diabatic cooling (Matsuno, 1966; Gill, 1980; Hu et al., 2022a). The above reduced rainfall and anomalous easterly winds are consistent with the delayed ISM onset associated precipitation and circulation anomalies (Fig. 4b). As outlined in many previous studies, the firm establishment of low-level southwesterly winds over the Arabian Sea is a prerequisite for ISM onset (Joseph et al., 2006; Pai and Rajeevan, 2009; Wang et al., 2009). The anomalous easterly winds in the Arabian Sea hinder the establishment of monsoonal southwesterly winds and moisture transport, thereby resulting in delayed ISM onset. Hence, this pattern further confirms the connection between the May North Pacific VM and ISM onset, i.e., the former tends to delay ISM onset.

3.2. *Dynamic mechanisms linking the VM and ISM onset*

The above analysis confirms that there is indeed a statistically significant and robust linkage between the North Pacific VM and monsoon onset. The next and more important scientific question is as follows: by what mechanisms does the VM affect ISM onset? It has been previously revealed that the ENSO and PDO can modulate ISM onset through the anomalous Walker circulation (Hu et al., 2022a; Hu et al., 2023), and it has been recently suggested that the VM in May modulates monsoon onset over the South China Sea via large-scale divergent circulation (Hu et al., 2022b). Thus, Fig. 5 shows an examination of the velocity potential anomalies in the upper and lower troposphere associated with the North Pacific VM. Upper-level divergence is only significant to the northeast of the Hawaii Islands. Moreover, in the lower level, there occurs significant convergence between the dateline and 240°E, as well as significant divergence over the Indo-China Peninsula, South China Sea, Philippine Sea, and East China Sea. These large-scale vertical motions may be driven by the SST gradient in the Pacific Ocean. Notably, low-level divergence over the South China Sea and the Indo-China Peninsula can contribute to reduced rainfall therein. This can stimulate the equatorial Rossby wave response to the west, which leads to

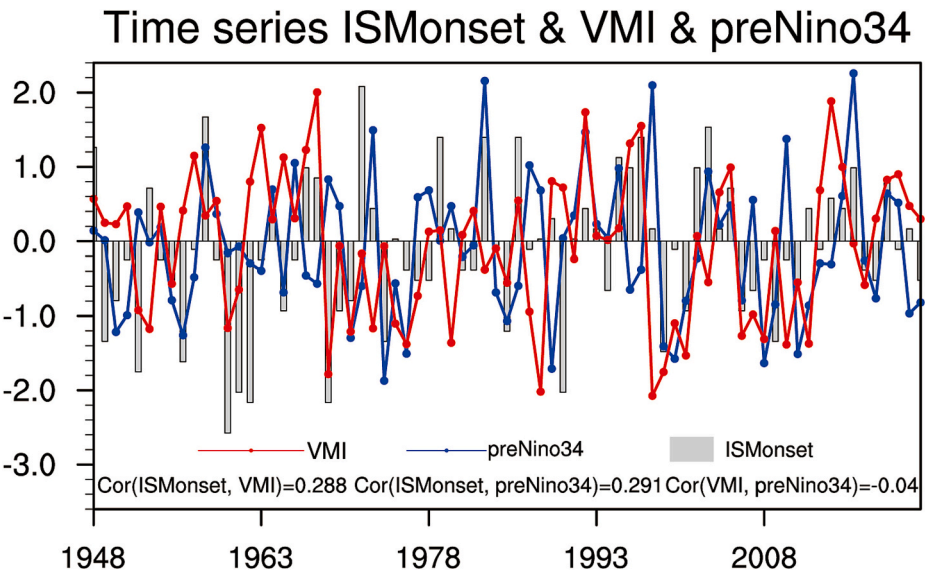

Fig. 3. The time series of normalized ISM onset date (gray bars), VM index in May (red line), and preceding winter Niño3.4 index (blue line). (For interpretation of the references to colour in this figure legend, the reader is referred to the web version of this article.)

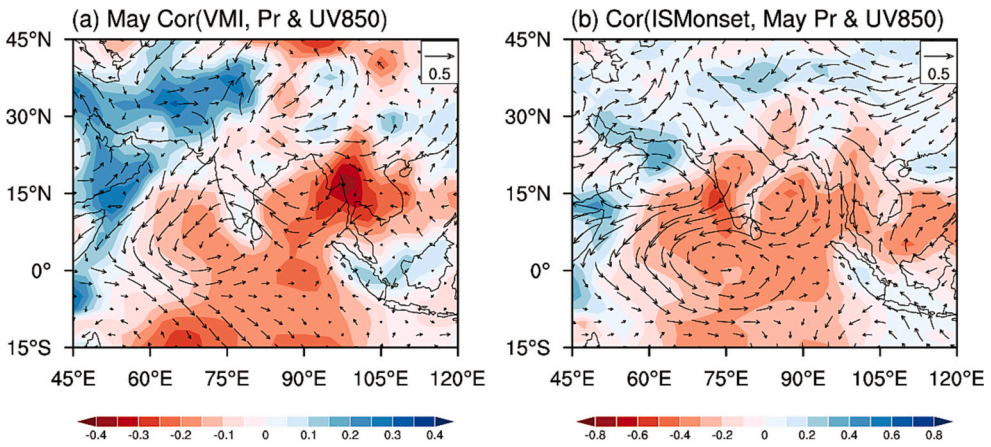

Fig. 4. (a) The correlation coefficient between May VM index and precipitation (shadings) and winds at 850 hPa (vectors). (b) The same as in (a), but for the ISM onset date and precipitation (shadings) and winds at 850 hPa (vectors).

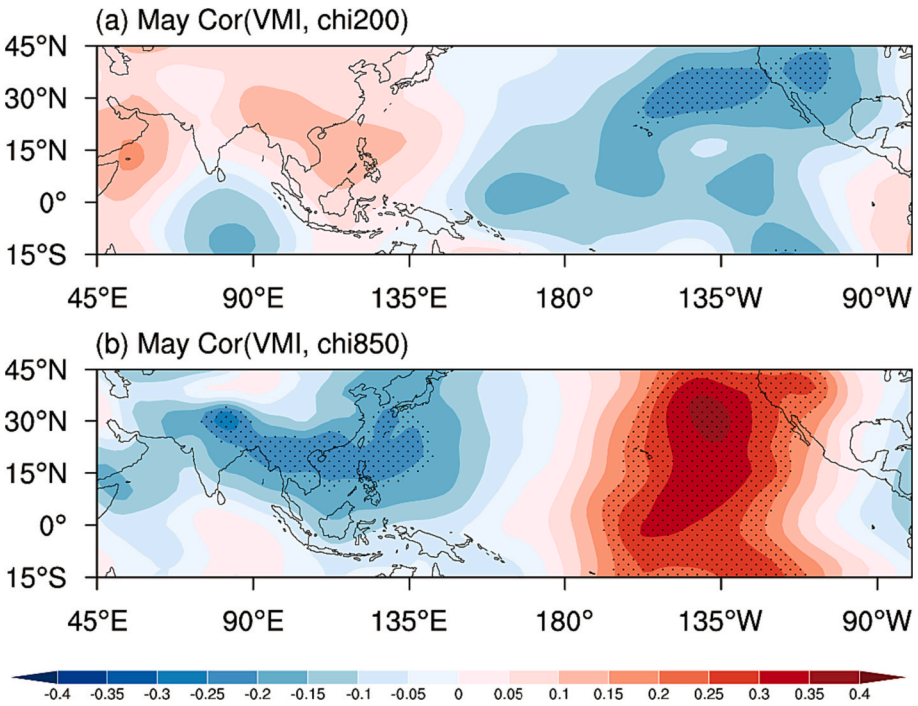

Fig. 5. The correlation coefficient between the May VMI and velocity potential at **(a)** 200 hPa, **(b)** 850 hPa. The dots denote the correlation coefficient passing the 90% confidence level.

anomalous easterly winds (Fig. 4). Such easterly winds prevent the firm establishment of monsoonal southwesterly winds and reduce water vapor transport from the Indian Ocean, thus contributing to delayed ISM onset. Therefore, we can conclude that, similar to the ENSO and PDO, the North Pacific VM can also modulate ISM onset through the tropical pathway, namely, large-scale divergent circulation and the equatorial Rossby wave response.

Given that another pathway in which the ENSO and PDO can modulate ISM onset involves the tropospheric temperature (Hu et al., 2022a; Hu et al., 2023), Fig. 6a shows an analysis of the temperature anomalies associated with the North Pacific VM. In sharp contrast to the ENSO and PDO, the temperature anomalies in the tropical region are rather weak and not significant. This probably occurs because the VM is primarily an extratropical mode, which does not exhibit significant SST anomalies except in the tropical central Pacific (Fig. 2c). However, alternating positive and negative air temperature anomalies emerge over the extratropics in the Northern Hemisphere. For example, warm air temperature anomalies are observed around the Hawaii Islands, Bering Sea, and Eastern Europe. In addition, cold air temperature anomalies emerge over the mid-latitude North Pacific, Eastern Canada and Greenland, and to the northwest of India. Notably, ISM circulation is largely driven by the land–sea thermal contrast, namely, the contrast between the warm Eurasian continent and the cold Indian Ocean (Webster et al., 1998; Chen et al., 2023; Hu et al., 2023; Lenka et al., 2023a). The cold airmass to the northwest of India induced by the positive phase of the VM in May reduces the meridional troposphere temperature gradient (Fig. 6b). Consequently, this reduced land–sea sea thermal contrast induces anomalous easterly winds and thus delays ISM onset.

The positive and negative temperature anomalies in the extratropics in the Northern Hemisphere suggest the possible existence of a Rossby wave train. To confirm this speculation, Fig. 7 shows the upper-level geopotential height anomalies regressed onto the VM index in May, as well as the associated wave activity fluxes (Takaya and Nakamura,

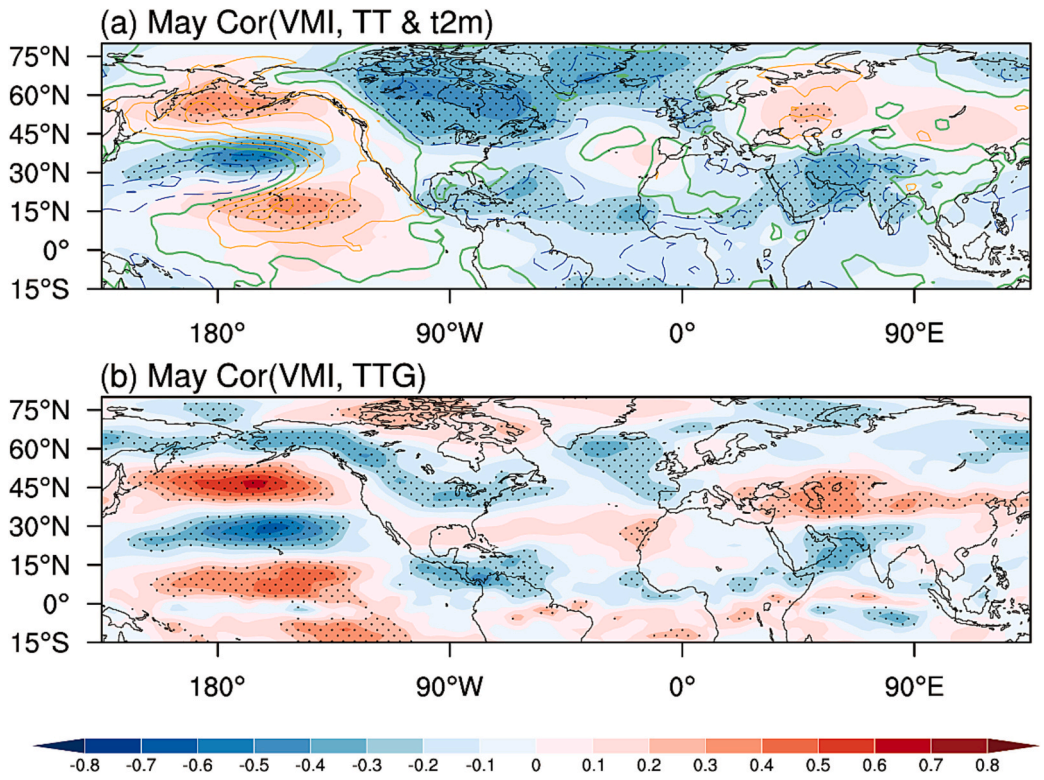

Fig. 6. (a) The correlation coefficient between the May VM index and troposphere temperature (TT; 850–200 hPa vertically averaged air temperature; shadings), and near-surface 2 m temperature (contours). (b) The same as in (a), but for the May VM index and meridional troposphere temperature gradient (TTG). The dots denote the correlation coefficient passing the 90% confidence level.

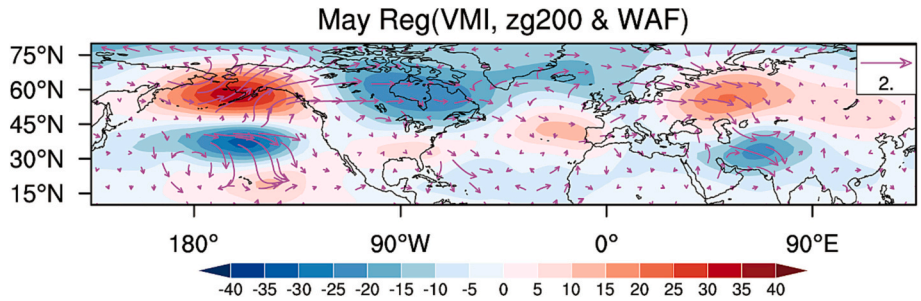

Fig. 7. Regression of the anomalous geopotential height at 200 hPa (shadings) and the associated wave activity flux (vectors) onto May VM index.

2001). The upper-tropospheric geopotential height anomalies correspond well to the temperature anomalies shown in Fig. 6, with cold (warm) air temperature anomalies conforming with negative (positive) geopotential height anomalies. For example, pronounced positive geopotential height anomalies occur over the Bering Sea, while negative geopotential height anomalies occur over the mid-latitude North Pacific. Such a dipole-like geopotential height pattern is referred to the North Pacific Oscillation/Western Pacific teleconnection pattern (Aru et al., 2021; Aru et al., 2022). The wave activity fluxes shown in Fig. 7 reveal two Rossby wave trains originating from the mid-latitude North Pacific. One is propagating southward and reaches the tropical Pacific, which is consistent with the recent study of Zhao et al. (2023a, 2023b). The other Rossby wave train begins by propagating northeastward, reaching North America, passing through the North Atlantic and Europe, and arriving in northwestern India. The anomalous low pressure in northwest India results in local cold air temperature anomalies, thus affecting the land–sea thermal contrast and ISM onset.

How does the VM excite the above Rossby wave train? Fig. 8a shows the regression pattern of the mid-tropospheric vertical velocity and upper-tropospheric Rossby wave source onto the May VM. A pronounced ascending motion and notable upper-level divergence emerge in the Gulf of Alaska. This divergence forms a strong Rossby wave source and may trigger the stationary Rossby wave train (Sardeshmukh and Hoskins, 1988; Hu et al., 2017). To confirm the important role of this Rossby wave source, upper-level divergence forcing over (50°-60°N, 205°-225°E) is prescribed in the LBM. Fig. 8b shows the steady atmospheric response, and an extratropical Rossby wave train can be observed. Despite several small differences, certain important observational features are captured by the LBM. For example, the negative geopotential height in the subtropical North Pacific and the positive geopotential height in the Gulf of Alaska are clearly observed. In particular, the negative geopotential height in northwest India is captured by the LBM. As previously mentioned, such geopotential height anomalies result in low temperatures and reduce the land–sea thermal contrast. Thus, in addition to the aforementioned tropical pathway, the North Pacific VM can modulate ISM onset through an extratropical pathway, namely, the Rossby wave train and meridional temperature gradient.

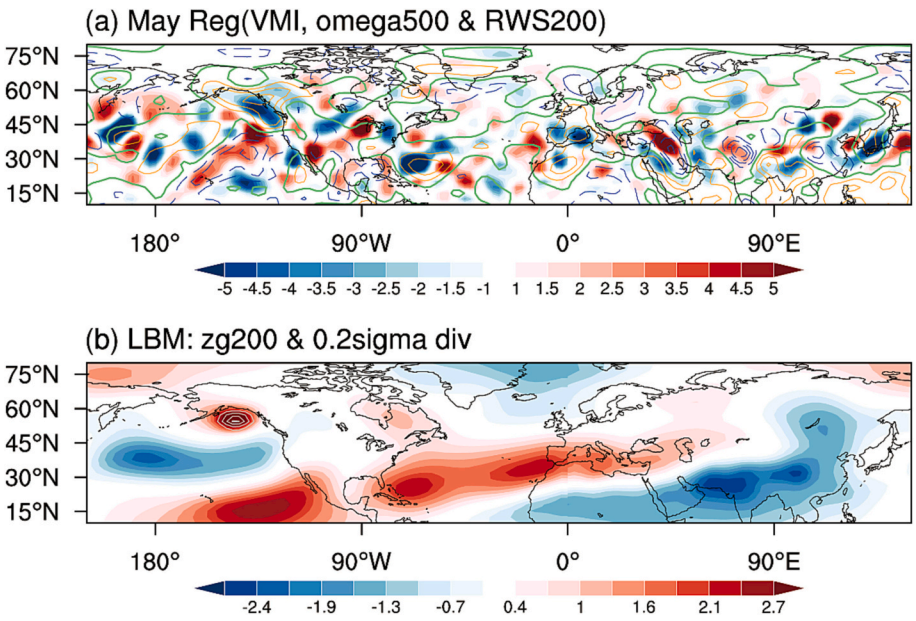

Fig. 8. (a) Regression of the vertical velocity at 500 hPa (contours) and Rossby wave source at 200 hPa (shadings) onto May VMI. **(b)** The steady response of geopotential height at 200 hPa (shadings; units: m) in the LBM, which is forced by the idealized upper-level divergence (gray contours; units: 10^{-5} s^{-1}) in the Gulf of Alaska (50°-60°N, 205°-225°E). The zonal mean geopotential height is removed to highlight the Rossby wave train.

4. Summary and discussion

In previous work, the importance of preceding ENSO events for ISM onset has been noted, which mainly involves tropical pathways. Based on reanalysis datasets and model simulations, in this study, we investigated the statistical relationship and the dynamic mechanisms linking the North Pacific VM and ISM onset. The positive phase of the VM, featuring cold SST anomalies in the mid-latitude North Pacific sandwiched by warm SST anomalies to both the south and north, is conducive to delayed ISM onset. As summarized in Fig. 9, the North Pacific VM modulates ISM onset via two distinct mechanisms: the tropical pathway and the extratropical pathway. Specifically, the SST gradient in the Pacific Ocean associated with the VM induces low-level convergence in the tropical central Pacific and divergences over the Indo-China Peninsula and WNP. This low-level divergence results in reduced rainfall, which serves as diabatic cooling forcing and excites the equatorial Rossby wave response to the west. The anomalous easterly winds to the south of the anticyclone hinder the establishment of monsoonal southwesterly winds and moisture transport, thus resulting in delayed ISM onset.

In addition, the North Pacific VM is accompanied by North Pacific Oscillation-like geopotential height anomalies in the upper-level, which excite a Rossby wave train that propagates downstream. This extratropical Rossby wave train can yield negative geopotential height anomalies and cold air temperature anomalies to the northwest of India, which can reduce the climatological land–sea thermal contrast. Therefore, the seasonal transition in the meridional temperature gradient and ISM onset is delayed. Notably, the tropical pathway predominantly carries the signal westward, while the extratropical pathway mainly carries the signal eastward. Due to the spherical nature of the Earth, the VM signals carried along these two pathways intersect in the Indian region and jointly modulate ISM onset.

The above conclusion is based on monthly average data, as daily or pentad precipitation data for the 1951–2022 period are not available. When utilizing the exact ISM onset date, the in-phase relationship between the May VM and ISM onset remains robust. Fig. S2 shows the correlation between the May VM index and 850 hPa winds and the tropospheric temperature averaged over the 23 May–07 June period. This three-pentad duration includes one standard deviation (7.3 days) before and after the mean ISM onset date (31 May), which is more closely linked to monsoon onset. Notably, the results shown in Fig. S2 (23 May–07 June) closely resemble those shown in Figs. 4a and 6a

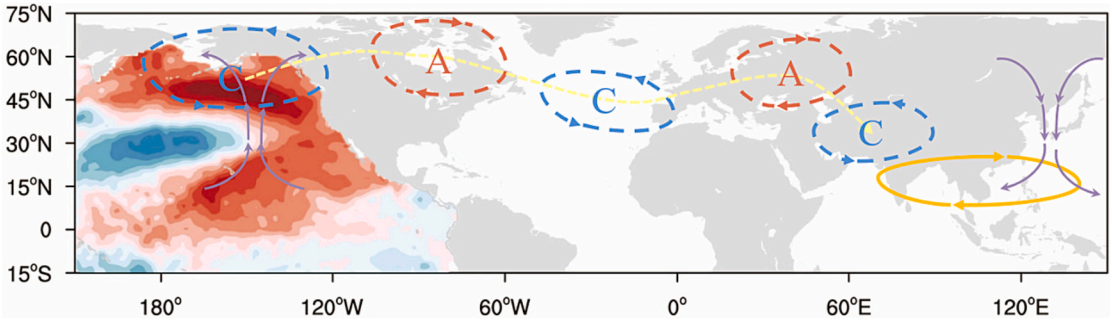

Fig. 9. The schematic diagram shows the two different mechanisms considered in this study, by which the May VM affects the ISM onset. Red (blue) shadings indicate the May VM-associated SST anomalies. The tropical pathway: purple arrows present the large-scale divergent circulation; orange anticyclone represents the tropical Rossby wave response to the decreased rainfall over the Indo-China Peninsula. The extratropical pathway: red anticyclones and blue cyclones with yellow dashed line denote the stationary Rossby wave train. (For interpretation of the references to colour in this figure legend, the reader is referred to the web version of this article.)

(May). Namely, the close relationship between the VM in May and anomalous low-level easterly winds extends from the Bay of Bengal to the Arabian Sea (Figs. S2a and 4a), and the extratropical geopotential height anomalies associated with the Rossby wave train (Figs. S2b and 6a). In addition, several researchers investigated monsoon onset using monthly mean data of May (Xiang and Wang, 2013; Watanabe and Yamazaki, 2014; Hu et al., 2022a, 2022b; Hu et al., 2023). In conclusion, the suitability of monthly mean data for analyzing monsoon onset depends on the scientific question considered. Monthly mean fields may not be adequate for those examining high-frequency disturbances on the exact date of monsoon onset. However, for researchers focusing on the modulation of large-scale circulation on interannual monsoon onset (i.e., advanced or delayed), monthly mean data can be appropriate (Xiang and Wang, 2013; Watanabe and Yamazaki, 2014; Hu et al., 2022a, 2022b; Hu et al., 2023).

In this study, we clarified two distinct mechanisms through which the May North Pacific VM affects ISM onset: the tropical Rossby response and the extratropical stationary Rossby wave train. This is an extension of the work of Hu et al. (2022a), who investigated the impact of the PDO on Asian summer monsoon onset. However, as outlined in the Introduction, the VM and PDO are the first two modes of North Pacific variability, and they are orthogonal and linearly independent of each other. Consequently, exploring the connection between the VM and ISM onset is very important for enhancing the accuracy of monsoon onset predictions. Nonetheless, it should be noted that this study primarily relies on reanalysis and observational datasets. Thus, more sophisticated model simulations are imperative for validating above pathways and mechanisms, especially their relative contributions. Furthermore, in addition to the ENSO, PDO, and VM in the Pacific Ocean, the SST variability in the Indian Ocean is very prominent (Athira and Abhilash, 2020). For example, the Indian Ocean Dipole (IOD) can also modulate ISM onset (Sankar et al., 2011; Lenka et al., 2023a), which is characterized by out-of-phase variation in the SST anomalies between the tropical western and southeastern Indian Oceans (Saji et al., 1999; Cheng et al., 2023). Sankar et al. (2011) investigated the roles of the ENSO and IOD in controlling ISM onset and they noted that La Niña and negative IOD events are favorable for advanced monsoon onset. This underscores the need to explore the combined effect of the ENSO, IOD, and VM in the future.

Declaration of Competing Interest

The authors declare that they have no known competing financial interests or personal relationships that could have appeared to influence the work reported in this paper.

Data availability

The National Centers for Environmental Prediction/National Center for Atmospheric Research (NCEP/NCAR) reanalysis data is available from http://www.psl.noaa.gov/data/gridded/data.ncep.reanalysis.derived.html.

The Precipitation Reconstruction (PREC) data is available from https://www.psl.noaa.gov/data/gridded/data.prec.html.

The Hadley Centre Global Sea Ice and Sea Surface Temperature (HadISST) data is available from http://www.metoffice.gov.uk/hadobs/hadisst.

Acknowledgments

This study was supported by the National Natural Science Foundation of China (Grants 42141019, 41831175, 42205021, 91937302, and 41721004).

Ethics approval and consent to participate

Not applicable.

Consent for publication

Written information consent for publication was obtained from all participants.

Credit authorship contribution statement

Suqin Zhang: Data curation, Investigation, Formal analysis, Software, Validation, Writing – original draft. **Peng Hu:** Conceptualization, Methodology, Formal analysis, Writing – review & editing, Funding acquisition. **Gang Huang:** Supervision, Writing – review & editing, Funding acquisition, Project administration. **Xia Qu:** Supervision, Writing – review & editing.

Appendix A. Supplementary data

Supplementary data to this article can be found online at https://doi.org/10.1016/j.atmosres.2023.107126.

References

Baburaj, P.P., Abhilash, S., Abhiram Nirmal, C.S., Sreenath, A.V., Mohankumar, K., Sahai, A.K., 2022a. Increasing incidence of Arabian Sea cyclones during the monsoon onset phase: its impact on the robustness and advancement of Indian summer monsoon. Atmos. Res. https://doi.org/10.1016/j.atmosres.2021.105915.

Ananthakrishnan, R., Soman, M.K., 1988. The onset of the southwest monsoon over Kerala: 1901–1980. J. Clim. 8, 283–296. https://doi.org/10.1002/joc.3370080305.

Aru, H., Chen, W., Chen, S., 2021. Is there any Improvement in simulation of the Wintertime Western Pacific Teleconnection Pattern and Associated climate Anomalies in CMIP6 compared to CMIP5 Models? J. Clim. 34, 8841–8861. https://doi.org/10.1175/JCLI-D-21-0016.1.

Aru, H., Chen, S., Chen, W., 2022. Change in the variability in the Western Pacific pattern during boreal winter: roles of tropical Pacific Sea surface temperature anomalies and North Pacific storm track activity. Clim. Dyn. 58, 2451–2468. https://doi.org/10.1007/s00382-021-06014-1.

Athira, U.N., Abhilash, S., 2020. Ocean-Atmosphere coupled processes in the Tropical Indian Ocean Region prior to Indian Summer Monsoon Onset over Kerala. Clim. Dyn. https://doi.org/10.1007/s00382-020-05499-6.

Baburaj, P.P., Abhilash, S., Vijaykumar, P., Abhiram Nirmal, C.S., Mohankumar, K., Sahai, A.K., 2022b. Concurrent cyclogenesis in the Northern Indian Ocean and Monsoon Onset over Kerala in response to different MJO phases. Atmos. Res. https://doi.org/10.1016/j.atmosres.2022.106435.

Bawiskar, S.M., 2009. Weakening of lower tropospheric temperature gradient between Indian landmass and neighbouring oceans and its impact on Indian monsoon. J Earth Syst Sci 118, 273–280. https://doi.org/10.1007/s12040-009-0029-2.

Bombardi, R.J., Kinter, J.L., Frauenfeld, O.W., 2019. A Global Gridded Dataset of the Characteristics of the Rainy and Dry Seasons. Bull. Am. Meteorol. Soc. 100, 1315–1328. https://doi.org/10.1175/BAMS-D-18-0177.1.

Bombardi, R.J., Moron, V., Goodnight, J.S., 2020. Detection, variability, and predictability of monsoon onset and withdrawal dates: a review. Int. J. Climatol. 40, 641–667. https://doi.org/10.1002/joc.6264.

Bond, N.A., Overland, J.E., Spillane, M., Stabeno, P., 2003. Recent shifts in the state of the North Pacific. Geophys. Res. Lett. 30, 2183. https://doi.org/10.1029/2003GL018597.

Chen, M., Xie, P., Janowiak, J.E., Arkin, P.A., 2002. Global Land Precipitation: a 50-yr Monthly Analysis based on Gauge Observations. J. Hydrometeorol. 3, 249–266. https://doi.org/10.1175/1525-7541(2002)003<0249:GLPAYM>2.0.CO;2.

Chen, S., Yu, B., Wu, R., Chen, W., Song, L., 2021. The dominant North Pacific atmospheric circulation patterns and their relations to Pacific SSTs: historical simulations and future projections in the IPCC AR6 models. Clim. Dyn. 56, 701–725. https://doi.org/10.1007/s00382-020-05501-1.

Chen, W., Zhang, R., Wu, R., Wen, Z., et al., 2023. Recent advances in Understanding Multi-scale climate Variability of the Asian Monsoon. Adv. Atmos. Sci. 40, 1429–1456. https://doi.org/10.1007/s00376-023-2266-8.

Cheng, X., Chen, S., Chen, W., et al., 2023. Observed impact of the Arctic Oscillation in boreal spring on the Indian Ocean Dipole in the following autumn and possible physical processes. Clim. Dyn. 61 (1–2), 883–902.

Chiang, J.C.H., Sobel, A.H., 2002. Tropical Tropospheric Temperature Variations Caused by ENSO and their Influence on the Remote Tropical climate. J. Clim. 15, 2616–2631. https://doi.org/10.1175/1520-0442(2002)015<2616:Tttvcb>2.0.Co;2.

Dai, Y., Wang, B., Wei, N., Song, J., Duan, Y., 2022. How has the North Pacific Gyre Oscillation affected peak season tropical cyclone genesis over the western North Pacific from 1965 to 2020? Environ. Res. Lett. 17, 104016 https://doi.org/10.1088/1748-9326/ac89a1.

Deepa, R., Oh, J.H., 2014. Indian summer monsoon onset vortex formation during recent decades. Theor. Appl. Climatol. 118, 237–249. https://doi.org/10.1007/s00704-013-1057-z.
Deser, C., Alexander, M.A., Xie, S.P., Phillips, A.S., 2010. Sea Surface Temperature Variability: patterns and Mechanisms. Annu. Rev. Mar. Sci. 2, 115–143. https://doi.org/10.1146/annurev-marine-120408-151453.
Ding, R., Li, J., Tseng, Y.H., Sun, C., Guo, Y., 2015. The Victoria mode in the North Pacific linking extratropical sea level pressure variations to ENSO. J. Geophys. Res. Atmos. 120, 27–45. https://doi.org/10.1002/2014JD022221.
Ding, R., Li, J., Tseng, Y.H., Li, L., Sun, C., Xie, F., 2018. Influences of the North Pacific Victoria mode on the South China Sea summer monsoon. Atmosphere 9, 229. https://doi.org/10.3390/atmos9060229.
Ding, R., Tseng, Y.H., Di, Lorenzo. E., Shi, L., Li, J., Yu, J.Y., Wang, C., Sun, C., Luo, J.J., Ha, K.J., 2022. Multi-year El Niño events tied to the North Pacific Oscillation. Nat. Commun. 13, 3871. doi: https://doi.org/10.1038/s41467-022-31516-9.
Gill, A.E., 1980. Some simple solutions for heat-induced tropical circulation. Q. J. R. Meteorol. Soc. 106, 447–462. https://doi.org/10.1002/qj.49710644905.
Goswami, P., Gouda, K.C., 2010. Evaluation of a dynamical basis for advance forecasting of the date of onset of monsoon rainfall over India. Mon. Weather Rev. 138 (8), 3120–3141.
Gouda, K.C., Joshi, S., Bhat, N., 2021. An optimum initial manifold for improved skill and lead in long-range forecasting of monsoon variability. Theor. Appl. Climatol. 144, 1161–1170. https://doi.org/10.1007/s00704-021-03589-x.
Hu, K., Huang, G., Wu, R., Wang, L., 2017. Structure and dynamics of a wave train along the wintertime Asian jet and its impact on East Asian climate. Clim. Dyn. 51, 4123–4137. https://doi.org/10.1007/s00382-017-3674-1.
Hu, P., Chen, W., Chen, S., Liu, Y., Huang, R., 2020. Extremely early Summer Monsoon Onset in the South China Sea in 2019 following an El Niño Event. Mon. Weather Rev. 148, 1877–1890. https://doi.org/10.1175/mwr-d-19-0317.1.
Hu, K., Huang, G., Huang, P., Kosaka, Y., Xie, S.P., 2021. Intensification of El Niño-induced atmospheric anomalies under greenhouse warming. Nat. Geosci. 14, 377–382. https://doi.org/10.1038/s41561-021-00730-3.
Hu, P., Chen, W., Chen, S., Liu, Y., Wang, L., Huang, R., 2022a. The leading Mode and Factors for Coherent Variations among the Subsystems of Tropical Asian Summer Monsoon Onset. J. Clim. 35, 1597–1612. https://doi.org/10.1175/JCLI-D-21-0101.1.
Hu, P., Chen, W., Chen, S., Wang, L., Liu, Y., 2022b. The weakening Relationship between ENSO and the South China Sea Summer Monsoon Onset in recent decades. Adv. Atmos. Sci. 39, 443–455. https://doi.org/10.1007/s00376-021-1208-6.
Hu, P., Chen, W., Chen, S., Wang, L., Liu, Y., 2023. Impacts of Pacific Ocean SST on the interdecadal variations of tropical Asian summer monsoon onset: new eastward-propagating mechanisms. Clim. Dyn. https://doi.org/10.1007/s00382-023-06824-5.
Ji, K., Tseng, Y., Ding, R., Mao, J., Feng, L., 2023. Relative contributions to ENSO of the seasonal footprinting and trade wind charging mechanisms associated with the Victoria mode. Clim. Dyn. 60, 47–63. https://doi.org/10.1007/s00382-022-06300-6.
Joseph, P.V., Eischeid, J., Pyle, R.J., 1994. Interannual Variability of the Onset of the Indian Summer Monsoon and its Association with Atmospheric Features, El Niño, and Sea Surface Temperature Anomalies. J. Clim. 7, 81–105. https://doi.org/10.1175/1520-0442(1994)007<0081:IVOTOO>2.0.CO;2.
Joseph, P.V., Sooraj, K.P., Rajan, C.K., 2006. The summer monsoon onset process over South Asia and an objective method for the date of monsoon onset over Kerala. Int. J. Climatol. 26, 1871–1893. https://doi.org/10.1002/joc.1340.
Kalnay, E., Kanamitsu, M., Kistler, R., Collins, W., et al., 1996. The NCEP/NCAR 40-Year Reanalysis Project. Bull. Am. Meteorol. Soc. 77, 437–472. https://doi.org/10.1175/1520-0477(1996)077<0437:TNYRP>2.0.CO;2.
Kikuchi, K., 2021. The boreal summer intraseasonal oscillation (BSISO): a review. J. Meteorol. Soc. Jpn. 99, 933–972. https://doi.org/10.2151/jmsj.2021-045.
Krishnamurti, T.N., Ardanuy, P., Ramanathan, Y., Pasch, R., 1981. On the onset vortex of the summer monsoon. Mon. Weather Rev. 109, 344–363. https://doi.org/10.1175/1520-0493(1981)109<0344:OTOVOT>2.0.CO;2.
Lee, J.Y., Wang, B., Wheeler, M.C., Fu, X., Waliser, D.E., Kang, I.S., 2013. Real-time multivariate indices for the boreal summer intraseasonal oscillation over the Asian summer monsoon region. Clim. Dyn. 40, 493–509. https://doi.org/10.1007/s00382-012-1544-4.
Lenka, S., Gouda, K.C., Devi, R., et al., 2023a. Dynamics of Indian summer monsoon in different phases. Clim. Dyn. https://doi.org/10.1007/s00382-023-06925-1 online at.
Lenka, S., Gouda, K.C., Devi, R., et al., 2023b. Dynamical Influence of MJO Phases on the Onset of Indian Monsoon. Environ. Res. Commun. 5, 061006.
Li, T., Wang, B., Wu, B., Zhou, T., Chang, C.P., Zhang, R., 2017. Theories on formation of an anomalous anticyclone in western North Pacific during El Niño: a review. J. Meteorol. Res. 31, 987–1006. https://doi.org/10.1007/s13351-017-7147-6.
Li, J., Zheng, F., Sun, C., Feng, J., Wang, J., 2019. Pathways of Influence of the Northern Hemisphere Mid-high Latitudes on East Asian climate: a Review. Adv. Atmos. Sci. 36, 902–921. https://doi.org/10.1007/s00376-019-8236-5.
Liu, Z., Di Lorenzo, E., 2018. Mechanisms and Predictability of Pacific Decadal Variability. Curr. Clim. Change. Rep. 4, 128–144. https://doi.org/10.1007/s40641-018-0090-5.
Liu, B., Zhu, C., 2021. Subseasonal-to-seasonal predictability of onset dates of South China Sea summer monsoon: a perspective of meridional temperature gradient. J. Clim. 34 (13), 5601–5616.
Matsuno, T., 1966. Quasi-geostrophic motions in the equatorial area. J. Meteorol. Soc. Jpn. 44, 25–43. https://doi.org/10.2151/jmsj1965.44.1_25.
Newman, M., Alexander, M.A., Ault, T.R., Cobb, K.M., et al., 2016. The Pacific Decadal Oscillation. Revisited. J. Clim. 29, 4399–4427. https://doi.org/10.1175/jcli-d-15-0508.1.
Noska, R., Misra, V., 2016. Characterizing the onset and demise of the Indian summer monsoon. Geophys. Res. Lett. 43, 4547–4554. https://doi.org/10.1002/2016GL068409.
Ordoñez, P., Gallego, D., Ribera, P., Peña-Ortiz, C., García-Herrera, R., 2016. Tracking the Indian Summer Monsoon Onset Back to the Preinstrument Period. J. Clim. 29, 8115–8127. https://doi.org/10.1175/jcli-d-15-0788.1.
Pai, D.S., Rajeevan, M.N., 2009. Summer monsoon onset over Kerala: New definition and prediction. J. Earth System Sci. 118, 123–135. https://doi.org/10.1007/s12040-009-0020-y.
Preenu, P.N., Joseph, P.V., Dineshkumar, P.K., 2017. Variability of the date of monsoon onset over Kerala (India) of the period 1870–2014 and its relation to sea surface temperature. J. Earth System Sci. 126, 76. https://doi.org/10.1007/s12040-017-0852-9.
Pu, X., Chen, Q., Zhong, Q., Ding, R., Liu, T., 2019. Influence of the North Pacific Victoria mode on western North Pacific tropical cyclone genesis. Clim. Dyn. 52, 245–256. https://doi.org/10.1007/s00382-018-4129-z.
Qian, Y., Hsu, P.C., Kazuyoshi, K., 2019. New real-time indices for the quasi-biweekly oscillation over the Asian summer monsoon region. Clim. Dyn. 53, 2603–2624. https://doi.org/10.1007/s00382-019-04644-0.
Rayner, N., Parker, D.E., Horton, E., Folland, C.K., Alexander, L.V., Rowell, D., Kent, E., Kaplan, A., 2003. Global analyses of sea surface temperature, sea ice, and night marine air temperature since the late nineteenth century. J. Geophys. Res.-Atmos. 108, 4407. https://doi.org/10.1029/2002JD002670.
Saji, N.H., Goswami, B.N., Vinayachandran, P.N., et al., 1999. A dipole mode in the tropical Indian Ocean. Nature 401 (6751), 360–363.
Sankar, S., Kumar, M.R.R., Reason, C., 2011. On the relative roles of El Nino and Indian Ocean Dipole events on the Monsoon Onset over Kerala. Theor. Appl. Climatol. 103, 359–374.
Sardeshmukh, P., Hoskins, B., 1988. The generation of global rotational flow by steady idealized tropical divergence. J. Atmos. Sci. 45, 1228–1251. https://doi.org/10.1175/1520-0469(1988)045<1228:TGOGRF>2.0.CO;2.
Sasanka, T., Osuri, K.K., Niyogi, D., 2023. Machine learning and dynamics based error-index method for the detection of monsoon onset vortex over the Arabian Sea: Climatology and composite structures. Q. J. R. Meteorol. Soc. 149, 537–555. https://doi.org/10.1002/qj.4422.
Takaya, K., Nakamura, H., 2001. A Formulation of a Phase-Independent Wave-activity Flux for Stationary and Migratory Quasigeostrophic Eddies on a Zonally varying Basic Flow. J. Atmos. Sci. 58, 608–627. https://doi.org/10.1175/1520-0469(2001)058<0608:Afoapi>2.0.Co;2.
Wang, B., Wu, R., Fu, X., 2000. Pacific–East Asian teleconnection: How does ENSO affect East Asian climate? J. Clim. 13, 1517–1536. https://doi.org/10.1175/1520-0442(2000)013<1517:PEATHD>2.0.CO;2.
Wang, B., Ding, Q., Joseph, P.V., 2009. Objective Definition of the Indian Summer Monsoon Onset. J. Clim. 22, 3303–3316. https://doi.org/10.1175/2008JCLI2675.1.
Wang, B., Li, J., He, Q., 2017. Variable and robust East Asian monsoon rainfall response to El Niño over the past 60 years (1957–2016). Adv. Atmos. Sci. 34, 1235–1248. https://doi.org/10.1007/s00376-017-7016-3.
Watanabe, M., Kimoto, M., 2000. Atmosphere-ocean thermal coupling in the North Atlantic: a positive feedback. Q. J. R. Meteorol. Soc. 126, 3343–3369. https://doi.org/10.1002/qj.49712657017.
Watanabe, T., Yamazaki, K., 2014. Decadal-Scale Variation of South Asian Summer Monsoon Onset and its Relationship with the Pacific Decadal Oscillation. J. Clim. 27, 5163–5173. https://doi.org/10.1175/JCLI-D-13-00541.1.
Webster, P.J., Magana, V.O., Palmer, T., Shukla, J., Tomas, R., Yanai, M., Yasunari, T., 1998. Monsoons: Processes, predictability, and the prospects for prediction. J. Geophy. Res. Oce. 103, 14451–14510. https://doi.org/10.1029/97JC02719.
Wheeler, M.C., Hendon, H.H., 2004. An all-season real-time multivariate MJO index: Development of an index for monitoring and prediction. Mon. Weather Rev. 132, 1917–1932. doi: 10.1175/1520-0493(2004)132<1917:AARMMI>2.0.CO;2.
Wilks, D.S., 2019. Statistical Methods in the Atmospheric Sciences, vol. Elsevier. United States, Cambridge.
Wu, X., Mao, J., 2019. Decadal changes in Interannual Dependence of the Bay of Bengal Summer Monsoon Onset on ENSO Modulated by the Pacific Decadal Oscillation. Adv. Atmos. Sci. 36, 1404–1416. https://doi.org/10.1007/s00376-019-9043-8.
Xiang, B., Wang, B., 2013. Mechanisms for the advanced Asian summer monsoon onset since the mid-to-late 1990s. J. Clim. 26, 1993–2009. https://doi.org/10.1175/JCLI-D-12-00445.1.
Xie, S.P., Kosaka, Y., Du, Y., Hu, K., Chowdary, J.S., Huang, G., 2016. Indo-western Pacific Ocean capacitor and coherent climate anomalies in post-ENSO summer: a review. Adv. Atmos. Sci. 33, 411–432. https://doi.org/10.1007/s00376-015-5192-6.
Yang, Y., Su, Q., Wang, L., Yang, R., Cao, J., 2022. Response of the South Asian High in May to the early spring North Pacific Victoria Mode. J. Clim. 35, 3979–3993. https://doi.org/10.1175/JCLI-D-21-0665.1.
Yu, W., Liu, Y., Xu, L., Wu, G., Yang, S., Chen, D., Yang, X.Q., Hu, C., He, B., 2022. Potential impact of spring thermal forcing over the tibetan plateau on the following winter el niño–southern oscillation. Geophys. Res. Lett. 49 https://doi.org/10.1029/2021GL097234 e2021GL097234.
Zhang, W., Leung, Y., Min, J., 2013. North Pacific Gyre Oscillation and the occurrence of western North Pacific tropical cyclones. Geophys. Res. Lett. 40, 5205–5211. https://doi.org/10.1002/grl.50955.
Zhang, J.Y., Wang, L., Yang, S., Chen, W., Huangfu, J., 2016. Decadal changes of the wintertime tropical tropospheric temperature and their influences on the

extratropical climate. Sci. Bull. 61, 737–744. https://doi.org/10.1007/s11434-016-1054-6.
Zhang, R., Min, Q., Su, J., 2017. Impact of El Niño on atmospheric circulations over East Asia and rainfall in China: Role of the anomalous western North Pacific anticyclone. Sci. China Earth Sci. 60, 1124–1132. https://doi.org/10.1007/s11430-016-9026-x.
Zhang, S., Qu, X., Huang, G., Hu, P., 2023. Asymmetric response of south Asian summer monsoon rainfall in a carbon dioxide removal scenario. Npj Clim. Atmos. Sci. 6, 6–10. https://doi.org/10.1038/s41612-023-00338-x.
Zhao, J., Sung, M.K., Park, J.H., Luo, J.J., Kug, J.S., 2023a. Part I observational study on a new mechanism for North Pacific Oscillation influencing the tropics. npj Clim. Atmos. Sci. 6, 15. https://doi.org/10.1038/s41612-023-00336-z.
Zhao, J., Sung, M.K., Park, J.H., Luo, J.J., Kug, J.S., 2023b. Part II model support on a new mechanism for North Pacific Oscillation influence on ENSO. npj Clim. Atmos. Sci. 6, 16. https://doi.org/10.1038/s41612-023-00337-y.
Zou, Q., Ding, R., Li, J., Tseng, Y.H., Hou, Z., Wen, T., Ji, K., 2020. Is the North Pacific Victoria Mode a Predictor of Winter Rainfall over South China? J. Clim. 33, 8833–8847. https://doi.org/10.1175/jcli-d-19-0789.1.